ELSEVIER

Journal of Organometallic Chemistry 530 (1997) 19–25

Journal of Organometallic Chemistry

Substituent effects on the cyclo-manganation reaction X-ray crystal structure of $Mn\{2\text{-}(^{n}Bu\text{-}N{=}CH)5\text{-}(NO_2)C_6H_3\}(CO)_4$

Colin Morton, David J. Duncalf, Jonathan P. Rourke *

Department of Chemistry, Warwick University, Coventry CV4 7AL, UK

Received 21 February 1996; revised 19 July 1996

Abstract

The cyclometallation reaction between methylmanganese pentacarbonyl and a number of Schiff's bases has been studied. The dependence of the rate of reaction upon ligand substituents has been investigated, demonstrating a rate enhancement with more electron-rich ligands.

The X-ray structure of $Mn\{2\text{-}(^{n}Bu\text{-}N{=}CH)5\text{-}(NO_2)C_6H_3\}(CO)_4$ has been determined.

Keywords: Cyclometallation; Manganese; Carbonyl

1. Introduction

Much work has been performed upon cyclometallation: a variety of review articles testify to this [1–4]. Previously, the emphasis has often been on the preparation of the cyclometallated species and their subsequent use in organic synthesis. Recently, however, cyclometallated species have attracted attention for their materials properties. In particular, cyclopalladated compounds have been much used as liquid crystals [5–15]. The dominance of cyclopalladated complexes in this area is not complete: a solitary example of cyclomanganated liquid crystal exists [16], with one further report of the rhenium analogue [17]. Our own work on cyclomanganated complexes concerns their potential use as materials for non-linear optics (NLO). In the course of this work, we have sought to synthesise a number of cyclomanganated complexes containing a variety of different electronic density distributions within the molecule. In the process we have succeeded in synthesising and characterising a number of compounds that it had been suggested were impossible to make. We were also able to establish some valuable insights into the mechanism of the cyclomanganation reaction, the mechanism of which has aroused a certain amount of discussion. Early reports by Bruce et al. of cyclomanganation with $RMn(CO)_5$ (R = Me and Bz) suggested that it was clear that the manganese species was behaving in a nucleophilic fashion [18], whereas a subsequent report from Sales and coworkers suggested that the mechanism was one whereby the manganese species behaved as an electrophile [19].

2. Results and discussion

2.1. Synthesis and characterisation of the complexes

Scheme 1 indicates the general synthetic route used to prepare our cyclomanganated complexes from Schiff's base ligands. The Schiff's bases that we used were substituted in either the para (compounds **1**) or meta (compounds **2**) positions with either methoxy (compounds **a**) or nitro (compounds **b**) groups. When compounds **1** cyclometallate only one product is possible, i.e. compounds **3**. However, when compounds **2** cyclometallate, two isomeric forms are possible: compounds **4** and **5**.

All six possible compounds (**3a**, **3b**, **4a**, **4b**, **5a** and **5b**) were successfully synthesised, final purification and separation of compounds **4** and **5** being achieved by column chromatography. In all cases, the total yield was respectable (65–85%).

Spectroscopic characterisation was performed on all complexes. Proton NMR spectra showed no unexpected features, with all peaks being fully assigned; data are to

* Corresponding author. Tel.: (+44) 1203 523263; fax: (+44) 1203 524112; e-mail: j.rourke@warwick.ac.uk.

PII S0022-328X(96)06663-6

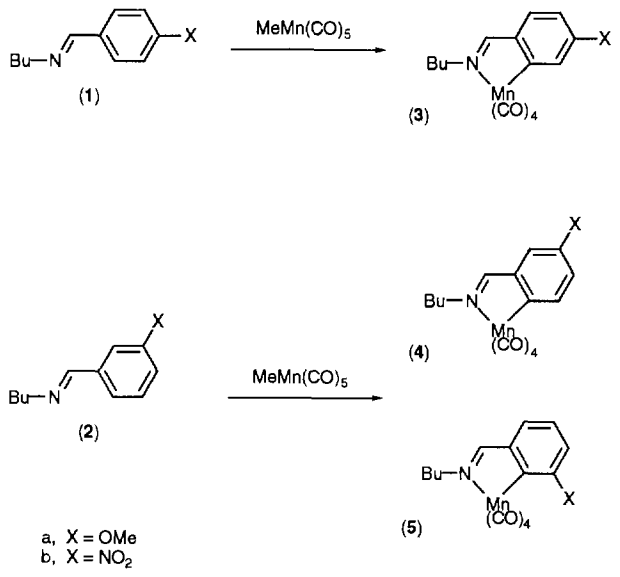

Scheme 1.

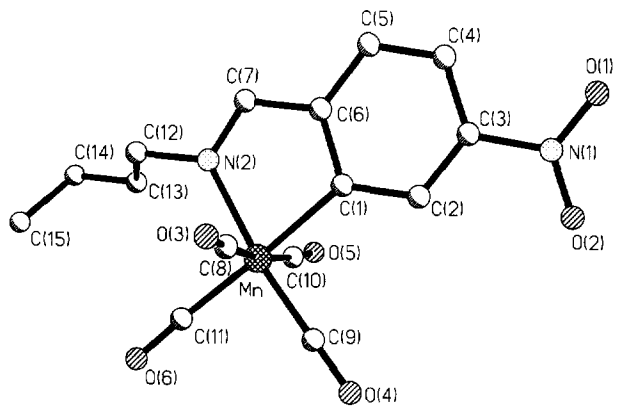

Fig. 1. Crystal structure of **3b**. Only one component of the disordered side chain (C(12)–C(15)) is shown.

be found in Section 4. IR spectra of the carbonyl region showed the expected four band pattern for the molecule: data are to be found in Table 1. An immediate difference between the methoxy (compounds **a**) and the nitro compounds (compounds **b**) is apparent: the stretching frequencies of the carbonyls are some 8–10 cm^{-1} higher in the case of the nitro compounds. This can very simply be explained in terms of the lower electron density present on the manganese in the case of the more electron withdrawing nitro ligand, leading to less back-bonding to the carbonyls, thus raising their stretching frequencies. The carbonyl stretching frequencies of all three nitro compounds were essentially identical, indicating very similar electronic and physical structures. In contrast, the stretching frequencies of the methoxy compounds show a significant variation between the isomers: whilst compounds **3a** and **4a** have essentially identical IR stretches, compound **5a** shows a clear difference. This difference has already been noted, and has been shown to arise from a real spatial interaction between the oxygen of the methoxy group and the carbon of the cis carbonyl [20].

Satisfactory elemental analyses were obtained for all six compounds: data are to be found in Table 1.

An X-ray structural determination was performed upon compound **3b**. Suitable crystals were grown from a THF solution. Refinement resulted in an R value of 0.0649. A view of the molecular structure of compound **3b** is shown in Fig. 1. The structure shows no unexpected features: the manganese is coordinated in a distorted octahedral configuration with the five-membered cyclomanganated ring, the aromatic ring and the nitro group being essentially planar. Table 2 lists positional parameters and ESDs; Table 3 lists principal bond lengths and angles; full data is available from the Cambridge Crystallographic Database. The pattern of observed bond lengths and angles are very similar to those others have obtained [20,21], though the length of the bond between manganese and the carbonyl carbons are significantly different. Comparing **3b** with its non-nitrated analogue, a significant manganese to carbonyl carbon bond length increase is observed — a mean increase of 0.046 Å across all four bonds, with one difference of 0.070 Å [21]. This increased bond length can simply be attributed to the electron withdrawing properties of the nitro group, which decreases the back-bonding to the carbonyls. It is interesting to note that this nitro-substituted compound is exactly the type of compound that others had suggested was impossible to make via this route [19].

The relative distribution of the two isomers (**4** and **5**) that are formed when ligands **2** are used can be determined from the integrations in the proton NMR of the crude reaction mixtures. When the methoxy ligand **2a** is

Table 1
Yields, IR and microanalytical data of the complexes

Compound	Yield/%	IR (THF sol.)/cm^{-1}	Microanalysis (expected)/%
3a	85	2072(w), 1987(s), 1974(m), 1932(m)	C 53.4 (53.8), H 4.8 (4.5), N 3.6 (3.9)
4a	22	2072(w), 1986(s), 1974(m), 1932(m)	C 53.7 (53.8), H 4.2 (4.5), N 3.6 (3.9)
5a	57	2071(w), 1984(s), 1977(m), 1936(m)	C 53.6 (53.8), H 4.3 (4.5), N 3.6 (3.9)
3b	72	2079(w), 1995(s), 1985(m), 1943(m)	C 48.2 (48.4), H 3.9 (3.5), N 7.2 (7.5)
4b	55	2079(w), 1995(s), 1986(m), 1943(m)	C 48.4 (48.4), H 3.8 (3.5), N 7.4 (7.5)
5b	10	2079(w), 1995(s), 1986(m), 1943(m)	C 48.3 (48.4), H 3.9 (3.5), N 7.1 (7.5)

Table 2
Atomic coordinates ($\times 10^4$) and equivalent isotropic displacement parameters ($Å^2 \times 10^3$) for **3b**

	x	y	z	U_{eq} [a]
Mn(1)	2133.9(6)	844.4(5)	4917.0(13)	32(1)
O(1)	6033(3)	2241(3)	1176(8)	73(2)
O(2)	4924(3)	2972(3)	2236(8)	62(1)
O(3)	1358(4)	606(3)	897(7)	65(2)
O(4)	1793(4)	2615(3)	4710(8)	67(2)
O(5)	3246(3)	999(3)	8608(7)	55(1)
O(6)	306(3)	626(3)	6704(7)	57(1)
N(1)	5270(4)	2313(4)	1884(8)	49(2)
N(2)	2543(4)	−361(3)	4833(7)	39(1)
C(1)	3394(4)	961(3)	3693(8)	30(1)
C(2)	3898(4)	1649(4)	3143(9)	37(1)
C(3)	4759(4)	1561(4)	2357(8)	33(1)
C(4)	5155(4)	813(4)	2008(9)	42(2)
C(5)	4685(4)	117(4)	2539(9)	41(2)
C(6)	3829(4)	198(4)	3388(8)	36(1)
C(7)	3313(4)	−499(4)	4045(9)	39(2)
C(8)	1633(4)	697(4)	2432(11)	43(2)
C(9)	1922(4)	1921(4)	4804(9)	40(2)
C(10)	2801(4)	951(4)	7261(9)	36(1)
C(11)	1020(4)	681(4)	6016(9)	38(2)
C(12)	2024(5)	−1053(4)	5599(12)	55(2)
C(13)	2015(6)	−1024(5)	7763(13)	68(2)
C(14A)	1578(10)	−1727(8)	8858(24)	76(5)
C(15A)	539(12)	−1680(10)	8494(26)	103(7)
C(14B)	1281(17)	−1726(14)	8111(35)	66(8)
C(15B)	1074(21)	−1634(18)	10230(36)	93(12)

[a] U_{eq} is defined as one-third of the trace of the orthogonalised U_{ij} tensor.

used, the dominant product is **5a**, the ratio of **5a** to **4a** being approximately 2.6. When the nitro ligand **2b** is used, the dominant product is **4b**, the ratio of **4b** to **5b** being approximately 5.5. These observations are not unexpected and fit with established precedents: the methoxy compound **5a** is stabilised by the interaction of the methoxy group with a cis carbonyl, this interaction being sufficient to overcome any unfavourable steric interactions [20]. In the case of the nitro compounds there is no such favourable interaction and steric factors dominate, producing the excess of **4b**. The relative ratios of the differing isomers found in the crude reaction mixture were reflected in the relative amounts of pure compounds collected after column chromatography.

In order to try and establish whether any equilibria existed between the isomers, separate samples of the pure compounds **4a**, **4b**, **5a** and **5b** were dissolved in THF and refluxed under an inert atmosphere overnight. NMR spectra were recorded: whilst some unidentified decomposition products were observed, none of the compounds isomerised to any of the other compounds. This is in contrast to other analogous systems, where it was clear that an equilibrium existed between the isomers, and indeed where it proved impossible to isolate the pure compounds [20].

GC-MS was used to demonstrate that the only by-product of the reaction was ethanal.

2.2. Kinetic runs

In order to arrive at a better understanding of the mechanism of the cyclomanganation reaction, a number of kinetic runs were performed. Reactions were carried out under an inert atmosphere in refluxing THF. Samples were removed for IR analysis: the quantity of starting material ($MeMn(CO)_5$) was monitored via the dominant 2008 cm^{-1} A_1 stretch. Throughout all the kinetic runs, the only compounds that were detectable, by IR, were the starting material and the product. The levels of product were found to mirror the levels of starting material, but were found to be less suitable for monitoring for kinetic purposes as the products decompose slowly under the experimental conditions. This decomposition was observed by taking separate samples of the pure compounds **3a** and **3b** and refluxing in THF: after 3 h IR indicated that approximately 5% of **3a** and 10% of **3b** had disappeared. In contrast, $MeMn(CO)_5$ showed no such decomposition.

In the first instance, the four different ligands (**1a**, **1b**, **2a** and **2b**) were reacted with $MeMn(CO)_5$ under pseudo first-order conditions: a ligand to Mn ratio of 10:1 was used (runs 1 to 4 respectively). A good first-order fit was observed in all cases, allowing a pseudo first-order rate constant to be determined: these are tabulated in Table 4.

In the second instance, the ligands **1a** and **1b** were reacted with $MeMn(CO)_5$ with a ligand to Mn ratio of 1:1 (runs 5 and 6 respectively). With ligand **1a** (run 5) a good first order fit was observed, whereas for ligand **1b** (run 6) the fit was not good. A second order fit was

Table 3
Principal bond lengths (Å) and angles (deg) for complex **3b** with ESDs in parentheses

Mn(1)–C(9)	1.792(7)	Mn(1)–C(11)	1.828(6)
Mn(1)–C(8)	1.869(8)	Mn(1)–C(10)	1.873(7)
Mn(1)–C(1)	2.047(6)	Mn(1)–N(2)	2.064(5)
O(4)–C(9)	1.156(7)	O(5)–C(10)	1.120(7)
O(6)–C(11)	1.157(7)	N(2)–C(7)	1.279(8)
N(2)–C(12)	1.473(8)		
C(9)–Mn(1)–C(11)	90.7(3)	C(9)–Mn(1)–C(8)	91.6(3)
C(11)–Mn(1)–C(8)	93.6(3)	C(9)–Mn(1)–C(10)	91.5(3)
C(11)–Mn(1)–C(10)	94.0(3)	C(8)–Mn(1)–C(10)	171.7(3)
C(9)–Mn(1)–C(1)	92.4(2)	C(11)–Mn(1)–C(1)	176.9(2)
C(8)–Mn(1)–C(1)	86.3(2)	C(10)–Mn(1)–C(1)	85.9(2)
C(9)–Mn(1)–N(2)	171.9(2)	C(11)–Mn(1)–N(2)	97.4(2)
C(8)–Mn(1)–N(2)	87.1(2)	C(10)–Mn(1)–N(2)	88.7(2)
C(1)–Mn(1)–N(2)	79.5(2)	C(7)–N(2)–C(12)	118.9(5)
C(7)–N(2)–Mn(1)	115.8(4)	C(12)–N(2)–Mn(1)	125.3(4)
C(1)–C(6)–C(7)	114.3(5)	N(2)–C(7)–C(6)	117.6(6)
O(3)–C(8)–Mn(1)	177.7(6)	O(4)–C(9)–Mn(1)	179.0(6)
O(5)–C(10)–Mn(1)	175.8(5)	O(6)–C(11)–Mn(1)	176.0(6)

Table 4

Run	Ligand	Ligand:Mn	Fit	Pseudo first-order rate coefficient k /s^{-1} [a]
1	**1a**	10:1	0.995	6.14×10^{-5}
2	**1b**	10:1	0.998	3.26×10^{-5}
3	**2a**	10:1	0.995	1.72×10^{-4}
4	**2b**	10:1	0.991	6.87×10^{-5}
5	**1a**	1:1	0.996	4.51×10^{-5}
6	**1b**	1:1	0.974 [b]	2.19×10^{-5}

[a] Where $-d[MeMn(CO)_5]/dt = k[MeMn(CO)_5]$. [b] Analysis as a second-order reaction gave a fit of 0.980.

performed for run 6, this fit being marginally better: these data are also tabulated in Table 4.

It is immediately apparent that in every comparable case the rate of reaction of the methoxy compound was faster than the nitro compounds (comparing runs 1 with 2, 3 with 4 and 5 with 6). The ratio of rates is around two.

A comparison of reaction rates of the *para*-substituted ligands (**1**) with the *meta*-substituted ligands (**2**) (comparing runs 1 with 3 and 2 with 4) shows a two-fold rate increase on going from the *para* to the *meta*.

It is also apparent that reducing the ligand to manganese ratio from 10:1 to 1:1 results in a drop in reaction rate. In the case of ligand **1a** (run 5), the reaction remains first order (to a good approximation). In the case of ligand **1b** (run 6), a good first-order fit is no longer obtained, though the second-order fit is only marginally better.

3. Discussion

The mechanism of the cyclomanganation reaction has not been clearly elucidated: here, we make a few further observations.

Others have failed to synthesise compounds containing nitro groups that are analogous to those we have characterised [19]. These workers used octane as the reaction solvent and ascribed their failure to synthesise any cyclometallated derivatives to the electron withdrawing properties of the nitro group present in the ligand, invoking an electrophilic attack of the manganese species on the ligand, Fig. 2(a).

Clearly, we are able to refute the impossibility of synthesising any such nitro containing compounds. The most likely first step of the cyclomanganation reaction would seem to be the migration of the methyl group of $MeMn(CO)_5$ onto a carbonyl, generating a vacant coordination site, followed by coordination of the ligand (steps A and B, Scheme 2). This type of reaction is well known and occurs faster in coordinating solvents [22]. In addition, the detection of ethanal by GC-MS as a reaction by-product strongly supports this migratory insertion step. Thus, when we perform our cyclometallations in a coordinating solvent (THF) we find good yields under reasonable conditions.

In addition, our kinetic data provide evidence for a multi-step reaction mechanism with no clearly defined rate determining step:

At high free ligand concentrations (ten equivalents per manganese), the rate of reaction is pseudo first order and greater than at low free ligand concentrations (one equivalent). At low free ligand concentrations the reaction rate is not necessarily first order (indeed, in the case of run 6, the second-order fit is better than the first-order one). This implies that the free ligand is in some way involved in a step of the reaction that helps determine the overall rate of the reaction.

The kinetic data clearly indicate a faster reaction rate with the methoxy ligands (compounds **a**) compared with the nitro ligands (compounds **b**). This result is apparently in contrast to previous work which noted that cyclomanganation takes place at an electron deficient ring in preference to one which is electron rich [18]. This evidence of regioselectivity implies a nucleophilic attack by the manganese species on the ring, Fig. 2(b). It is possible to ascribe our increase in rate, as others

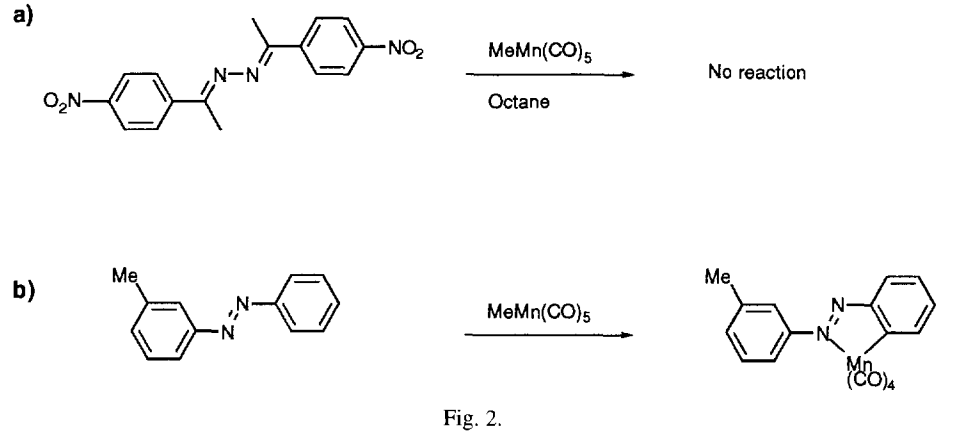

Fig. 2.

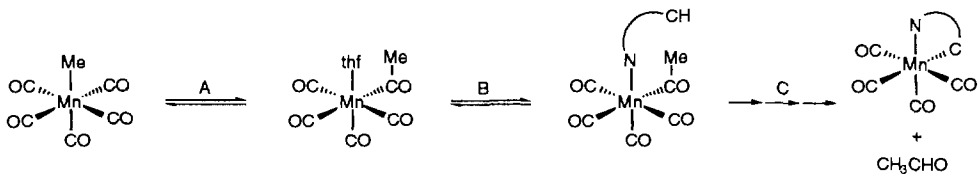

Scheme 2.

have, to the crucial reaction step being electrophilic attack by the manganese species on the ring [19].

It is clear to us that one of the first steps of the reaction must be coordination of the ligand, through the lone pair of the imine nitrogen, to the manganese. It is readily apparent that this will be more favourable with the more electron-rich system (e.g. methoxy substituted), compared with an electron deficient system (e.g. nitro substituted), and we propose that it is this difference that accounts for our observed difference in rate. The attack of the manganese upon the ring thus takes place at a subsequent stage of the reaction, and this must be a nucleophilic attack by the manganese on the ring, as previously reported [18].

Therefore, we propose the reaction mechanism outlined in Scheme 2.

It should also be noted that once a ligand has coordinated to the manganese, the more electron rich metal system (i.e. with the methoxy ligand) will be better set up to attack the ring in a nucleophilic manner than the less electron rich system (i.e. the nitro ligand). This facet of the reactivity was not taken into consideration by either of the sets of workers mentioned above [18,19], but has been noted by others [4].

The rate of reaction of the meta-substituted ligands (ligands **2**, runs 3 and 4) is faster for both the methoxy ligand (**2a**, run 3) and for the nitro case (**2b**, run 4), compared with the para-substituted ligands. In the case of the methoxy ligand (**2a**, run 3) the reaction rate increase is much greater (around a three-fold enhancement) and is almost certainly due to the additional thermodynamically favourable interaction of the methoxy group with a cis carbonyl on the manganese, which has already been noted [20]. One would not expect much of a difference between the ligating ability of the two methoxy ligands (compounds **1a** and **2a**): this is illustrated by the fact that compounds **3a** and **4a** have identical carbonyl stretching frequencies in the IR. Therefore, the rate of the reaction is being affected by the final cyclometallation step.

Thus, our results show that the reaction rate is affected by both the concentration of the free ligand (i.e. an initial coordination, steps A and B, Scheme 2) as well as by a subsequent reaction step involving a coordinated ligand (i.e. the nucleophilic attack by the manganese upon the ring, step C, Scheme 2). This leads us to the conclusion that there is no one true rate determining step in the cyclomanganation reaction, and that a number of the reaction steps occur at similar rates.

4. Experimental

4.1. General

All elemental analyses were performed by the Warwick University Microanalytical service. All NMR spectra were performed on a Bruker AC-250 in $CDCl_3$, and are referenced to external tetramethylsilane. IR spectra were performed on a Perkin–Elmer PE1710 FTIR. GC-MS experiments were performed on a Kratos MS-80, using a 50 m OV17 capillary column.

The $MeMn(CO)_5$ and all ligands were synthesised via literature routes [23,24]. THF was freshly distilled from molten potassium prior to use, all other chemicals were used as supplied.

4.2. Complex synthesis

All complexes were synthesised using the following general synthetic route.

Under an inert atmosphere, $MeMn(CO)_5$ (50 mg, 2.38×10^{-4} mol) and ligand **1a** (55 mg, 2.38×10^{-4} mol) were dissolved in THF (20 cm^3) and refluxed (16 h). The solvent was removed under vacuum to yield the crude product in 65–85% yield. Further purification and separation of any isomeric forms was effected by chromatography on silica using a dichloromethane–hexane (40/60) mixture as the elutant.

In one experiment, equimolar quantities of $MeMn(CO)_5$ and ligand **1a** were dissolved in THF and stirred at 5 °C for 48 h. A sample of the solution was removed and injected into the GC-MS. Ethanal was detected, whereas a control experiment with just $MeMn(CO)_5$ in THF showed no ethanal.

Yields, IR and microanalytical data are summarised in Table 1, NMR data are listed below; see Fig. 3.

4.2.1. Complex *3a*

δ_H: 8.11 (1H, s, H_e), 7.48 (1H, d, $^4J_{H-H}$ 1.5 Hz, H_h), 7.45 (1H, d, $^3J_{H-H}$ 8 Hz, H_f), 6.60 (1H, d, d, $^3J_{H-H}$ 8 Hz, $^4J_{H-H}$ 1.5 Hz, H_g), 3.89 (3H, s, OMe), 3.66 (2H, t, $^3J_{H-H}$ 7 Hz, H_d), 1.77 (2H, m, H_c), 1.31 (2H, m, H_b), 0.97 (3H, t, $^3J_{H-H}$ 7 Hz, H_a).

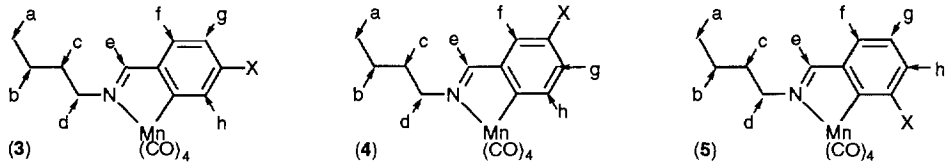

Fig. 3.

*4.2.2. Complex **3b***

δ_H: 8.74 (1H, d, $^4J_{H-H}$ 2 Hz, H_h), 8.34 (1H, s, H_e), 7.95 (1H, d, d, $^3J_{H-H}$ 7 Hz, $^4J_{H-H}$ 1.5 Hz, H_g), 7.66 (1H, d, $^3J_{H-H}$ 7 Hz, H_f), 3.80 (2H, t, $^3J_{H-H}$ 7 Hz, H_d), 1.85 (2H, m, H_c), 1.35 (2H, m, H_b), 1.00 (3H, t, $^3J_{H-H}$ 7 Hz, H_a).

*4.2.3. Complex **4a***

δ_H: 8.19 (1H, s, H_e), 7.79 (1H, d, $^3J_{H-H}$ 7.5 Hz, H_h), 7.14 (1H, d, $^4J_{H-H}$ 2.5 Hz, H_f), 6.96 (1H, d, d, $^3J_{H-H}$ 7.5 Hz, $^4J_{H-H}$ 2.5 Hz, H_g), 3.80 (3H, s, OMe), 3.72 (2H, t, $^3J_{H-H}$ 7 Hz, H_d), 1.80 (2H, m, H_c), 1.32 (2H, m, H_b), 0.98 (3H, t, $^3J_{H-H}$ 7 Hz, H_a).

*4.2.4. Complex **4b***

δ_H: 8.38 (1H, s, H_e), 8.30 (1H, d, $^4J_{H-H}$ 2 Hz, H_f), 8.18 (1H, d, $^3J_{H-H}$ 8 Hz, H_h), 8.06 (1H, d, d, $^3J_{H-H}$ 7.5 Hz, $^4J_{H-H}$ 2 Hz, H_g), 3.81 (2H, t, $^3J_{H-H}$ 7 Hz, H_d), 1.84 (2H, m, H_c), 1.37 (2H, m, H_b), 1.00 (3H, t, $^3J_{H-H}$ 7 Hz, H_a).

*4.2.5. Complex **5a***

δ_H: 8.22 (1H, s, H_e), 7.21 (1H, d, d, $^3J_{H-H}$ 7.5 Hz, $^4J_{H-H}$ 1.5 Hz, H_f), 7.14 (1H, t, $^3J_{H-H}$ 7.5 Hz, H_g), 6.79 (1H, d, d, $^3J_{H-H}$ 7.5 Hz, $^4J_{H-H}$ 1.5 Hz, H_h), 3.84 (3H, s, OMe), 3.72 (2H, t, $^3J_{H-H}$ 7 Hz, H_d), 1.81 (2H, m, H_c), 1.32 (2H, m, H_b), 0.97 (3H, t, $^3J_{H-H}$ 7 Hz, H_a).

*4.2.6. Complex **5b***

δ_H: 8.35 (1H, s, H_e), 7.66 (1H, d, d, $^3J_{H-H}$ 7.5 Hz, $^4J_{H-H}$ 1 Hz, $H_{f/h}$), 7.63 (1H, d, d, $^3J_{H-H}$ 7.5 Hz, $^4J_{H-H}$ 1 Hz, $H_{f/h}$), 7.27 (1H, t, $^3J_{H-H}$ 7.5 Hz, H_g), 3.81 (2H, t, $^3J_{H-H}$ 7 Hz, H_d), 1.84 (2H, m, H_c), 1.39 (2H, m, H_b), 1.02 (3H, t, $^3J_{H-H}$ 7 Hz, H_a)

*4.3. Crystal structure of **3b***

A crystal of **3b** suitable for X-ray analysis was grown from a THF solution.

*4.3.1. Crystal data for **3b***

$C_{15}H_{13}MnN_2O_6$, $M = 372.21$, monoclinic, space group $P2_1/c$, $a = 14.390(7)$ Å, $b = 16.401(6)$ Å, $c = 6.999(3)$ Å, $\alpha = 90°$, $\beta = 92.48(4)°$, $\gamma = 90°$, $U = 1650.3(12)$ Å^3, $Z = 4$, $D_c = 1.494$ g cm^{-3}, $F(000) = 756$, $\mu = 0.832$ mm^{-1}, crystal size $0.2 \times 0.45 \times 0.5$ mm^3.

4.3.2. General details

The crystal was held at 200 K with an Oxford Cryosystems Cryostream cooler. Scan speed 3–15° min^{-1} (ω), depending on the intensity of a 2 s pre-scan; backgrounds were measured at each end of the scan for 0.25 of the scan time. 3188 reflections were measured (independent reflections: 2930 (R(int) = 0.0456)) on a Siemens R3m diffractometer using graphite monochromated Mo Kα radiation (λ = 0.71073 Å, $50.10 > 2\theta > 4.96°$). Index ranges: $-17 \leq h \leq 17$, $-19 \leq k \leq 0$, $0 \leq l \leq 8$. The data were re-scaled to correct for any crystal decay (less than 2% variation in standards). Reflections were processed using profile analysis. Data were uncorrected for absorption and extinction.

Heavy atoms were located by the Patterson interpretation section of shelxtl [25] and the light atoms then found by F-map extension and successive Fourier syntheses.

Refinement: full-matrix least squares on F^2.

Anisotropic thermal parameters were used for all non-hydrogen atoms with the exception of C(14) and C(15); these were split into two, C(14A)–C(14B) and C(15A)–C(15B), with occupancy factors of 0.65 for each of C(14A) and C(15A) and 0.35 for each of C(14B) and C(15B). Hydrogen atoms were given fixed isotropic temperature factors, $U = 0.08$ Å^2. Those defined by the molecular geometry were inserted at calculated positions and not refined; the hydrogen atoms were allowed to ride on the parent atom (hydrogen atoms were not placed on the disordered C(14) and C(15), or C(13)).

$wR2 = \{\Sigma[w(F_o^2 - F_c^2)^2]/\Sigma[w(F_o^2)^2]\}^{1/2} = 0.2004$ (for all 3188 reflections), $R = \Sigma|F_o - F_c|/\Sigma F_o = 0.0649$ (2930 reflections with $I/2\sigma I > 2.0$). $S = 0.956$. 216 parameters. Weighting scheme $(W) = 1/[(F_o^2) + (0.1167P)^2 + 0.00P]$, where $P = [\max(F_o^2,0) + 2F_o^2]/3$ and $\max(F_o^2,0)$ indicates that the larger of F_o^2 or 0 is taken. Largest difference, peak and hole: 0.566 and -0.370 e Å^{-3}.

The positional parameters and ESDs are contained in Table 2, selected bond lengths and angles are in Table 3. All other data are available from the Cambridge Crystallographic Database.

4.4. Kinetic runs

In a typical kinetic run, a solution of ligand (2.38×10^{-3} mol) in THF ($1\,cm^3$) was added to a refluxing solution of $MeMn(CO)_5$ (50 mg, 2.38×10^{-4} mol) in THF ($9\,cm^3$), under an inert atmosphere. The solution was maintained at reflux, under an inert atmosphere for the duration of the experiment. An IR spectrum was run immediately, this reading taken to be $T = 0$. All the absorbance data relate to the intensity of the $2008\,cm^{-1}$ peak of the $MeMn(CO)_5$.

A series of kinetic runs were performed. Runs 1–4 utilised ligands **1a**, **1b**, **2a** and **2b** respectively at ten equivalents of ligand to one equivalent of $MeMn(CO)_5$. Runs 5 and 6 utilised ligands **1a** and **1b** respectively at one equivalent of ligand to one equivalent of $MeMn(CO)_5$. Derived rate coefficients are listed in Table 4.

Acknowledgements

We thank the University of Warwick Research and Teaching Innovations Fund for financial support (CM) and Dr. A. McCamley and Dr. C.J. Samuel for helpful discussions.

References

[1] J. Dehand and M. Pfeffer, *Coord. Chem. Rev., 18* (1976) 327.
[2] I. Omae, *Chem. Rev., 79* (1979) 287.
[3] A.D. Ryabov, *Synthesis*, (1985) 233.
[4] A.D. Ryabov, *Chem. Rev., 90* (1990) 403.
[5] J. Barberá, P. Espinet, E. Lalinde, M. Marcos and J.L. Serrano, *Liq. Cryst., 2* (1987) 833.
[6] P. Espinet, J. Pérez, M. Marcos, M.B. Ros, J.L. Serrano, J. Barberá and A.M. Levelut, *Organometallics, 9* (1990) 2028.
[7] P Espinet, E Lalinde, M Marcos, J Pérez and J L Serrano, *Organometallics, 9* (1990) 555.
[8] M.J. Baena, J. Barberá, P. Espinet, A. Ezcurra, M.B. Ros and J.L. Serrano, *J. Am. Chem. Soc., 116* (1994) 1899.
[9] N. Hoshino, H. Hasegawa and Y. Matsunaga, *Liq. Cryst., 9* (1991) 267.
[10] M. Marcos, J.L. Serrano, T. Sierra and M.J. Giménez, *Chem. Mater., 15* (1993) 1332.
[11] M. Ghedini, S. Morrone, G.D. Munno and A. Crispini, *J. Organomet. Chem., 415* (1991) 281.
[12] M. Ghedini, D. Pucci, E. Cesarotti, P. Antogniazza, O. Francescangeli and R. Bartolino, *Chem. Mater., 5* (1993) 883.
[13] M. Ghedini, D. Pucci, E. Cesarotti, O. Francescangeli and R. Bartolino, *Liq. Cryst., 16* (1994) 373.
[14] L. Zhang, D. Huang, N. Xiong, J. Yang, G. Li and N. Shu, *Mol. Cryst. Liq. Cryst., 237* (1993) 285.
[15] K. Praefcke, S. Diele, J. Pickardt, B. Gündogan, U. Nütz and D. Singer, *Liq. Cryst., 18* (1995) 857.
[16] D.W. Bruce and X.-H. Liu, *J. Chem. Soc. Chem. Commun.*, (1994) 729.
[17] D.W. Bruce and X.-H. Liu, *Liq. Cryst., 18* (1995) 165.
[18] M.I. Bruce, B.L. Goodall and F.G.A. Stone, *J. Chem. Soc. Dalton Trans.*, (1978) 687.
[19] R.M Ceder, J. Sales, X. Solans and M. Font-Altaba, *J. Chem. Soc. Dalton Trans.*, (1986) 1351.
[20] M. Pfeffer, E. Urriolabeitia and J. Fischer, *Inorg. Chem., 34* (1995) 643.
[21] R.G. Little and R.J. Doedens, *Inorg. Chem., 12* (1973) 840.
[22] F. Calderazzo, *Angew. Chem. Int. Ed. Engl., 16* (1977) 299.
[23] W. Beck and K. Raab, *Inorg. Synth., 28* (1990) 15.
[24] H. Weingarten, J.P. Chupp and W.A. White, *J. Org. Chem., 32* (1967) 3246.
[25] G.M. Sheldrick, SHELXL 93, University of Göttingen, 1993.